

Global dynamics of a discrete age-structured SIR epidemic model with applications to measles vaccination strategies[☆]



Linhua Zhou^a, Yan Wang^b, Yanyu Xiao^c, Michael Y. Li^{*,d}

^a Department of Applied Mathematics, Changchun University of Science and Technology, Changchun, Jilin 140022, PR China

^b School of Mathematical Sciences, Dalian University of Technology, Dalian, Liaoning 116023, PR China

^c Department of Mathematical Sciences, University of Cincinnati, Cincinnati, Ohio 45221, USA

^d Department of Mathematical and Statistical Sciences, University of Alberta, Edmonton, Alberta T6G 2G1, Canada

ARTICLE INFO

Keywords:

Epidemic models
Discrete age structure
Global stability
Measles vaccination

MSC:

34D20
92D30

ABSTRACT

We investigate an SIR epidemic model with discrete age groups to understand the transmission dynamics of an infectious disease in a host population with an age structure. We derive the basic reproduction number \mathcal{R}_0 and show that it is a sharp threshold parameter. If $\mathcal{R}_0 \leq 1$, the disease-free equilibrium E_0 is globally stable. If $\mathcal{R}_0 > 1$, E_0 is unstable, the model is uniformly persistent, and an endemic equilibrium exists. The global stability of the endemic equilibrium when $\mathcal{R}_0 > 1$ is established under a sufficient condition. The model is then used to analyze the measles data in India and evaluate the effectiveness of several vaccination strategies for the control of measles epidemics in India.

1. Introduction

Age distribution is one of the most important factors that contribute to the heterogeneity of populations and thus greatly influences the time course and outcomes of the transmission and spread of infectious diseases. Most importantly, patterns and frequencies of individual interactions can be drastically different among and across age groups and these differences produce a great degree of heterogeneity in transmission rates. Individuals at different age can also have different levels of immunity against infectious diseases. These differences can impact the age-specific mortality rates and recovery rates from an infection. Modeling the impact of age structure in a population on the transmission of an infectious disease is crucial for understanding the complexity of the disease dynamics and for effective disease control and prevention.

Age-structure in epidemic models has been studied using both discrete and continuous approaches in the literature. These studies include partial differential equation (PDE) models with continuous age structure (see a recent book [22] for references), and ordinary differential equation (ODE) models with discrete age groups (see e.g. [2,7,13]). For both approaches, the derivation of the basic reproduction number, the existence, uniqueness, and stability of equilibria are important issues.

For PDE models, well-posedness of models and properties of the associated semigroups have stimulated much of the recent theoretic development. For ODE models, while the mathematical framework is relatively simple due to its finite dimensional phase space, the challenge in their mathematical analysis lies in the high dimensionality and large-scale of the ODE system. In both approaches, it is highly nontrivial to establish the global dynamics of age-structured epidemic models. In particular, the uniqueness and global stability of the endemic equilibrium when the basic reproduction number exceeds one are very difficult mathematical problems.

Epidemic models with a discrete age structure can be regarded as coupled systems of nonlinear differential equations on transmission networks. In this setting, each age group can be considered as a node, and connections among nodes are defined by inter-group transmissions and the aging process. The graph-theoretic approach to the construction of Lyapunov functions for coupled systems on networks developed in [11,21] can be applied to models with discrete age groups. Such an approach was used in [18] to establish the global stability of the endemic equilibrium of an SIR model with discrete age structures in the susceptible population. The global stability of endemic equilibria of SIR epidemic models with discrete age structures in both susceptible and infectious populations are still an open problem. In this paper, we

* Submitted to the editors April 21, 2017.

Corresponding author.

E-mail addresses: zhoulh@cust.edu.cn (L. Zhou), wangy891@dlut.edu.cn (Y. Wang), yanyu.xiao@uc.edu (Y. Xiao), myli@ualberta.ca, mli@math.ualberta.ca (M.Y. Li).

present a new global-stability result to this problem using the approach in [11,21].

Studies on continuous age-structured epidemic models have shown that, when the basic reproduction number is greater than 1, uniqueness and global stability of the endemic equilibrium may not hold (see e.g. [3,8,28]). Investigations of similar results for discrete-structured epidemic models will be of interest. In our main result, global stability of the endemic equilibrium is proved under sufficient condition that holds for an open set of parameter values.

Vaccination is a major control measure against infectious diseases. One of the most common and successful vaccines is the measles vaccine, which is typically given to infants as part of the measles-mumps-rubella (MMR) vaccination. The efficacy of a single-dose of measles vaccine given to infants at 12 or 15 months of age is between 85% and 93%. A second dose is given before school age. With two doses, efficacy of measles vaccines can reach 97% [30]. Measles is one of the most serious infectious human diseases as it can cause severe illness, lifelong complications and death. By the estimation of the World Health Organization (WHO), even with routine vaccination programmes, millions of measles cases occur each year in developing countries [33], mainly due to low vaccination coverage. In its Global Measles and Rubella Strategic Plan: 2012–2020, WHO has set measles eradication targets for year 2020 for high measles incidence countries in Africa and Southeast Asia: a 95% or higher rate of vaccine coverage with both the first and second routine doses of measles vaccine, a reduction of the measles incidence rate to below 5 cases per million population, and a 95% reduction of measles mortality rate from that of year 2000 [34,35]. We adapted a discrete age-structured model to analyze measles data from India and examine the effects of the current vaccination programmes in India, which has the highest measles incidence rates in the world. We further discussed the effectiveness of different vaccination strategies for India in the context of WHO's measles elimination targets.

The organization of this paper is as follows: in Section 2, we formulate the discrete age-structured SIR epidemic model and derive the basic reproduction number \mathcal{R}_0 . In Section 3, we discuss the global stability of the disease-free equilibrium and the endemic equilibrium. In Section 4, we develop a vaccination model with four age groups to analyze different vaccination strategies for measles epidemics in India. We end the paper with conclusions and discussion in Section 5.

2. An SIR epidemic model with a discrete age structure

Partition the host population into n age groups. Each age group is further divided into three epidemiological classes: susceptible (S_k), infectious (I_k), and removed or immune (R_k). For the k th age group, Λ_k is the constant influx of susceptible, β_{kj} is the transmission coefficient between susceptible S_k and infectious I_j , d_k is the natural death rate, μ_k is the disease-caused death rate, γ_k is the recovery rate, and α_k is the rate for aging. The model is depicted in the transfer diagram in Fig. 1. Based on the transfer diagram, the model is described by the following system of ordinary differential equations:

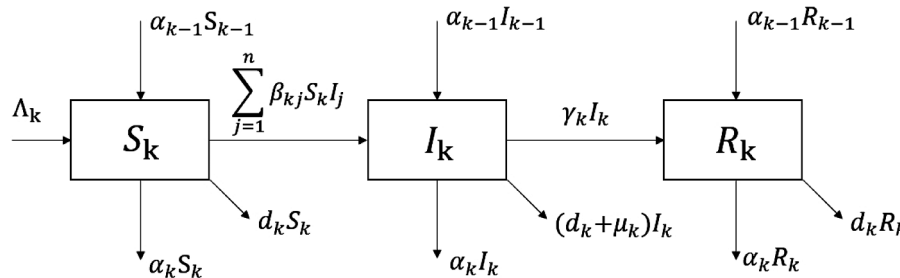


Fig. 1. Transfer diagram for the SIR model with a discrete age structure.

$$\begin{aligned} \frac{dS_k}{dt} &= \Lambda_k + \alpha_{k-1}S_{k-1} - \sum_{j=1}^n \beta_{kj}S_kI_j - d_kS_k - \alpha_kS_k, \\ \frac{dI_k}{dt} &= \alpha_{k-1}I_{k-1} + \sum_{j=1}^n \beta_{kj}S_kI_j - (d_k + \mu_k + \gamma_k + \alpha_k)I_k, \quad k = 1, 2, \dots, n. \\ \frac{dR_k}{dt} &= \alpha_{k-1}R_{k-1} + \gamma_kI_k - d_kR_k - \alpha_kR_k. \end{aligned} \quad (1)$$

Here, our convention for the aging is that $\alpha_0 = \alpha_n = 0$. We assume that $\Lambda_k \geq 0$, $\Lambda_1 > 0$, $d_k \geq 0$, and $d_n > 0$, for $k = 1, 2, \dots, n$. All other model parameters are assumed to be nonnegative.

Set $N_k = S_k + I_k + R_k$. It can be verified by adding the equations of S_k , I_k , R_k that, for $k = 1, 2, \dots, n$,

$$\limsup_{t \rightarrow \infty} N_k \leq (\Lambda_k + \alpha_{k-1}N_{k-1})/(d_k + \alpha_k) = :N_k^0. \quad (2)$$

Similarly, using the first equation of (1) we can derive, for $k = 1, 2, \dots, n$,

$$\limsup_{t \rightarrow \infty} S_k \leq (\Lambda_k + \alpha_{k-1}S_{k-1}^0)/(d_k + \alpha_k) = :S_k^0. \quad (3)$$

Observe that variable R_k does not appear in the first two equations of (1), and we can consider the following reduced system:

$$\begin{aligned} \frac{dS_k}{dt} &= \Lambda_k + \alpha_{k-1}S_{k-1} - \sum_{j=1}^n \beta_{kj}S_kI_j - d_kS_k - \alpha_kS_k, \\ \frac{dI_k}{dt} &= \alpha_{k-1}I_{k-1} + \sum_{j=1}^n \beta_{kj}S_kI_j - (d_k + \mu_k + \gamma_k + \alpha_k)I_k, \quad k = 1, 2, \dots, n. \end{aligned} \quad (4)$$

We investigate system (4) in the feasible region:

$$\Gamma = \{(S_1, I_1, \dots, S_n, I_n) \in \mathbb{R}_+^{2n} \mid 0 \leq S_k \leq S_k^0, S_k + I_k \leq N_k^0, k = 1, 2, \dots, n\}. \quad (5)$$

It can be shown that Γ is positively invariant with respect to (4).

System (4) always has the disease-free equilibrium $E_0 = (S_1^0, 0, S_2^0, 0, \dots, S_n^0, 0)$. Let

$$F = \begin{pmatrix} \beta_{11}S_1^0 & \beta_{12}S_1^0 & \cdots & \beta_{1n}S_1^0 \\ \beta_{21}S_2^0 & \beta_{22}S_2^0 & \cdots & \beta_{2n}S_2^0 \\ \vdots & \vdots & \ddots & \vdots \\ \beta_{n1}S_n^0 & \beta_{n2}S_n^0 & \cdots & \beta_{nn}S_n^0 \end{pmatrix}, \quad (6)$$

$$V = \begin{pmatrix} d_1 + \mu_1 + \gamma_1 + \alpha_1 & \cdots & 0 & 0 \\ -\alpha_1 & \cdots & 0 & 0 \\ \vdots & \ddots & \vdots & \vdots \\ 0 & \cdots & d_{n-1} + \mu_{n-1} + \gamma_{n-1} & 0 \\ & & + \alpha_{n-1} & \\ 0 & \cdots & -\alpha_{n-1} & d_n + \mu_n + \gamma_n + \alpha_n \end{pmatrix}. \quad (7)$$

Then using the method of van den Driessche and Watmough [32], the basic reproduction number, which measures the average number of

secondary infections caused by a single infectious individual in an entirely susceptible population during its infectious period, is given by

$$\mathcal{R}_0 = \rho(FV^{-1}), \quad (8)$$

where FV^{-1} is the next generation matrix and ρ denotes the spectral radius of a matrix. The following result follows from Theorem 2 of [32].

Proposition 1. *The disease-free equilibrium E_0 is local asymptotically stable if $\mathcal{R}_0 < 1$ and unstable if $\mathcal{R}_0 > 1$.*

3. Global dynamics of model (4)

Consider matrices:

$$F_1 = \begin{pmatrix} \beta_{11}S_1^0 & \beta_{12}S_1^0 & \cdots & \beta_{1n}S_1^0 \\ \beta_{21}S_2^0 + \alpha_1 & \beta_{22}S_2^0 & \cdots & \beta_{2n}S_2^0 \\ \beta_{31}S_3^0 & \beta_{32}S_3^0 + \alpha_2 & \cdots & \beta_{3n}S_3^0 \\ \vdots & \vdots & \ddots & \vdots \\ \beta_{n1}S_n^0 & \beta_{n2}S_n^0 & \cdots & \beta_{nn}S_n^0 \end{pmatrix}, \quad (9)$$

$$V_1 = \begin{pmatrix} d_1 + \mu_1 + \gamma_1 + \alpha_1 & 0 & \cdots & 0 \\ 0 & d_2 + \mu_2 + \gamma_2 + \alpha_2 & \cdots & 0 \\ \vdots & \vdots & \ddots & \vdots \\ 0 & 0 & \cdots & d_n + \mu_n + \gamma_n \end{pmatrix}, \quad (10)$$

and define

$$\mathcal{T}_0 = \rho(V_1^{-1}F_1). \quad (11)$$

Then we have the following result.

Proposition 2. $\text{sign}(\mathcal{R}_0 - 1) = \text{sign}(\mathcal{T}_0 - 1)$.

Proof. The result follows from the fact that $F - V = F_1 - V_1$. \square

3.1. Global stability of the disease-free equilibrium

Theorem 3. *Assume that $B = (\beta_{kj})_{n \times n}$ is irreducible. Then the following results hold.*

- (1) *If $\mathcal{R}_0 \leq 1$, then the disease-free equilibrium E_0 is the unique equilibrium of (4) and it is globally asymptotically stable in Γ ;*
- (2) *If $\mathcal{R}_0 > 1$, then the disease-free equilibrium E_0 is unstable, and system (4) is uniformly persistent in $\overset{\circ}{\Gamma}$. In particular, an endemic equilibrium E^* exists in $\overset{\circ}{\Gamma}$.*

Proof. Set $S = (S_1, S_2, \dots, S_n)^T$, $S^0 = (S_1^0, S_2^0, \dots, S_n^0)^T$, $I = (I_1, I_2, \dots, I_n)^T$, and define

$$M(S) = \begin{pmatrix} \beta_{ij}S_i + \alpha_{j-1}\delta_{(k-1)j} \\ d_i + \mu_i + \gamma_i + \alpha_i \end{pmatrix},$$

where δ_{st} is the Kronecker symbol such that $\delta_{st} = 1$ when $s = t$ and 0 when $s \neq t$. Then any equilibrium of system (4) satisfies the following matrix equation

$$M(S)I - I = 0.$$

From $M_0 = M(S^0) = V_1^{-1}F_1$ it follows $\mathcal{T}_0 = \rho(M_0)$. In the feasible region Γ , we have $0 \leq M(S) \leq M_0$ since $0 \leq S \leq S^0$. By properties of nonnegative matrices ([14]), we know that $M(S)$, M_0 and $M(S) + M_0$ are irreducible, and that $\rho(M(S)) < \rho(M_0)$ provided $S \neq S^0$. Therefore, if $\mathcal{T}_0 = \rho(M_0) \leq 1$ and $S \neq S^0$, we have $\rho(M(S)) < 1$ and $M(S)I - I = 0$ has only the trivial solution $I = 0$. Thus E_0 is the unique equilibrium of (4) in Γ if $\mathcal{T}_0 \leq 1$.

Since M_0 is nonnegative and irreducible, by Perron–Frobenius Theorem [4,14], $\mathcal{T}_0 = \rho(M_0) > 0$ is the dominant eigenvalue with a positive left eigenvector $(\omega_1, \omega_2, \dots, \omega_n)$. Set

$$l_k = \frac{\omega_k}{d_k + \mu_k + \gamma_k + \alpha_k},$$

and consider

$$L = \sum_{k=1}^n l_k I_k. \quad (12)$$

Differentiating L along solutions of system (4) we obtain

$$\begin{aligned} L' &= \sum_{k=1}^n l_k I'_k = \sum_{k=1}^n l_k (\alpha_{k-1}I_{k-1} + \sum_{j=1}^n \beta_{kj}S_k I_j - (d_k + \mu_k + \gamma_k + \alpha_k)I_k) \\ &= (l_1(d_1 + \mu_1 + \gamma_1 + \alpha_1), \dots, l_n(d_n + \mu_n + \gamma_n + \alpha_n))(M(S)I - I) \\ &= (\omega_1, \dots, \omega_n)(M(S)I - I) \\ &\leq (\omega_1, \dots, \omega_n)(M_0I - I) = (\omega_1, \dots, \omega_n)(\mathcal{T}_0 - 1)I \leq 0, \quad \text{if } \mathcal{T}_0 \leq 1. \end{aligned}$$

Furthermore, if $\mathcal{T}_0 < 1$, we have $L' = 0$ if and only if $I = 0$. If $\mathcal{T}_0 = 1$, then $L' = 0$ implies

$$(\omega_1, \dots, \omega_n)M(S)I = (\omega_1, \dots, \omega_n)I. \quad (13)$$

Since $S < S^0$ and $\rho(M(S)) < \mathcal{T}_0$, we find that equation (13) holds if and only if $I = 0$. Therefore, the largest invariant set in Γ where $L' = 0$ is the singleton $\{E_0\}$. By LaSalle's Invariance Principle [19], E_0 is globally asymptotically stable in Γ when $\mathcal{T}_0 \leq 1$.

If $\mathcal{T}_0 > 1$ and $I \neq 0$, we have

$$(\omega_1, \omega_2, \dots, \omega_n)M_0 - (\omega_1, \omega_2, \dots, \omega_n) = (\mathcal{T}_0 - 1)(\omega_1, \omega_2, \dots, \omega_n) > 0,$$

and by continuity,

$$L' = (\omega_1, \dots, \omega_n)(M(S)I - I) > 0$$

in a small neighborhood of E_0 in $\overset{\circ}{\Gamma}$. This implies that the disease-free equilibrium E_0 is unstable when $\mathcal{T}_0 > 1$. Based on a uniform persistence result in [9] and a similar argument as in the proof of Proposition 3.3 in [20], when $\mathcal{T}_0 > 1$, the uniform persistence of (4) is guaranteed by the instability of E_0 . The existence of E^* follows from the uniform persistence and uniform boundedness of solutions in Γ (see [6] or [27]). Using Proposition 2 we know that $\mathcal{R}_0 < 1$ if and only if $\mathcal{T}_0 < 1$, and the proof is complete. \square

3.2. Global stability and uniqueness of the endemic equilibrium

Denote an endemic equilibrium by

$$E^* = (S_1^*, I_1^*, S_2^*, I_2^*, \dots, S_n^*, I_n^*) \text{ in } \overset{\circ}{\Gamma}.$$

Let

$$\phi_{kj}^* = \beta_{kj}S_k^*I_j^* + \delta_{k-1,j}\alpha_{k-1}I_{k-1}^*$$

where $\delta_{i,j}$ is the Kronecker delta function, namely, $\delta_{i,j} = 1$ if $i = j$, otherwise $\delta_{i,j} = 0$, and set

$$\Phi = \begin{pmatrix} \sum_{i \neq 1} \phi_{i1}^* & -\phi_{21}^* & \cdots & -\phi_{n1}^* \\ -\phi_{12}^* & \sum_{i \neq 2} \phi_{2i}^* & \cdots & -\phi_{n2}^* \\ \vdots & \vdots & \ddots & \vdots \\ -\phi_{1n}^* & -\phi_{2n}^* & \cdots & \sum_{i \neq n} \phi_{ni}^* \end{pmatrix}. \quad (14)$$

Then, the following result is standard in linear algebra (see e.g., Lemma 2.1 in [11]).

Lemma 4. *Assume that $B = (\beta_{kj})_{n \times n}$ is irreducible. Then the following linear system*

$$\Phi v = 0,$$

has a positive solution (v_1, v_2, \dots, v_n) defined by

$$(v_1, v_2, \dots, v_n) = (C_{11}, C_{22}, \dots, C_{nn}), \quad (15)$$

where C_{kk} , $k = 1, 2, \dots, n$, denotes the cofactor of the k th diagonal entry of matrix Φ .

Theorem 5. Suppose that $B = (\beta_{kj})_{n \times n}$ is irreducible and that $\mathcal{R}_0 > 1$. Assume that the following conditions hold

$$d_k S_k^* + \alpha_k S_k^* - \alpha_{k-1} S_{k-1}^* - \frac{v_{k+1}}{v_k} \alpha_k S_k^* \geq 0, \quad k = 1, 2, \dots, n. \quad (16)$$

Then system (4) has a unique endemic equilibrium $E^* = (S_1^*, I_1^*, S_2^*, I_2^*, \dots, S_n^*, I_n^*)$ and it is globally asymptotically stable in $\overset{\circ}{\Gamma}$.

Proof. Let $v_k > 0$ be as given in (15) and $g(x) = x - 1 - \ln x$. Then, $g(x) \geq 0$ for $x > 0$ and $g(x) = 0$ if and only if $x = 1$. Set

$$V = V(S, I) = \sum_{k=1}^n v_k \left[S_k^* g\left(\frac{S_k}{S_k^*}\right) + I_k^* g\left(\frac{I_k}{I_k^*}\right) \right],$$

and let $V(t) = V(S(t), I(t))$ along a solution $(S(t), I(t))$ of (4). Then

$$\begin{aligned} V'(t) &= \sum_{k=1}^n v_k \left[S'_k - \frac{S'_k}{S_k} S_k^* + I'_k - \frac{I'_k}{I_k} I_k^* \right] \\ &= \sum_{k=1}^n v_k \left[\left(1 - \frac{S_k^*}{S_k}\right) [\Lambda_k + \alpha_{k-1} S_{k-1} - \sum_{j=1}^n \beta_{kj} S_k I_j - d_k S_k - \alpha_k S_k] \right. \\ &\quad \left. + \left(1 - \frac{I_k^*}{I_k}\right) [\alpha_{k-1} I_{k-1} + \sum_{j=1}^n \beta_{kj} S_k I_j - (d_k + \mu_k + \gamma_k + \alpha_k) I_k] \right] \\ &= \sum_{k=1}^n v_k \left[(d_k S_k^* + \alpha_k S_k^*) \left(2 - \frac{S_k}{S_k^*} - \frac{S_k^*}{S_k}\right) + \alpha_{k-1} S_{k-1} - \alpha_{k-1} S_{k-1}^* \right. \\ &\quad \left. + \alpha_{k-1} \frac{S_{k-1}^* S_k^*}{S_k} - \alpha_{k-1} \frac{S_{k-1} S_k^*}{S_k} + \alpha_{k-1} I_{k-1}^* \left(1 + \frac{I_{k-1}}{I_{k-1}^*} - \frac{I_k}{I_k^*} - \frac{I_k^* I_{k-1}}{I_k I_{k-1}^*}\right) \right. \\ &\quad \left. + \sum_{j=1}^n \beta_{kj} S_k^* I_j^* \left(2 - \frac{S_k}{S_k^*} - \frac{I_k}{I_k^*} + \frac{I_j}{I_j^*} - \frac{I_k^* I_j S_k}{I_k I_j^* S_k^*}\right) \right] \\ &= \sum_{k=1}^n v_k \left[\left(d_k S_k^* + \alpha_k S_k^* - \alpha_{k-1} S_{k-1}^* - \frac{v_{k+1}}{v_k} \alpha_k S_k^*\right) \left(2 - \frac{S_k}{S_k^*} - \frac{S_k^*}{S_k}\right) \right. \\ &\quad \left. + \alpha_{k-1} S_{k-1}^* \left(3 - \frac{S_k}{S_k^*} - \frac{S_{k-1}^*}{S_{k-1}} - \frac{S_{k-1} S_k^*}{S_k}\right) \right. \\ &\quad \left. + \alpha_{k-1} I_{k-1}^* \left(1 + \frac{I_{k-1}}{I_{k-1}^*} - \frac{I_k}{I_k^*} - \frac{I_k^* I_{k-1}}{I_k I_{k-1}^*}\right) \right. \\ &\quad \left. + \sum_{j=1}^n \beta_{kj} S_k^* I_j^* \left(2 - \frac{S_k}{S_k^*} - \frac{I_k}{I_k^*} + \frac{I_j}{I_j^*} - \frac{I_k^* I_j S_k}{I_k I_j^* S_k^*}\right) \right]. \end{aligned}$$

Using relations $2 - \frac{S_k}{S_k^*} - \frac{S_k^*}{S_k} \leq 0$, $3 - \frac{S_k}{S_k^*} - \frac{S_{k-1}^*}{S_{k-1}} - \frac{S_{k-1} S_k^*}{S_k} \leq 0$, for all $S_k > 0$, and assumption (16), we have

$$\begin{aligned} V'(t) &\leq \sum_{k=1}^n v_k \left[\alpha_{k-1} I_{k-1}^* \left(1 + \frac{I_{k-1}}{I_{k-1}^*} - \frac{I_k}{I_k^*} - \frac{I_k^* I_{k-1}}{I_k I_{k-1}^*}\right) \right. \\ &\quad \left. + \sum_{j=1}^n \beta_{kj} S_k^* I_j^* \left(2 - \frac{S_k}{S_k^*} - \frac{I_k}{I_k^*} + \frac{I_j}{I_j^*} - \frac{I_k^* I_j S_k}{I_k I_j^* S_k^*}\right) \right] \\ &= \sum_{k=1}^n v_k \left[\alpha_{k-1} I_{k-1}^* \left(g\left(\frac{I_{k-1}}{I_{k-1}^*}\right) - g\left(\frac{I_k}{I_k^*}\right) - g\left(\frac{I_k^* I_{k-1}}{I_k I_{k-1}^*}\right)\right) \right. \\ &\quad \left. + \sum_{j=1}^n \beta_{kj} S_k^* I_j^* \left(-g\left(\frac{S_k}{S_k^*}\right) - g\left(\frac{I_k}{I_k^*}\right) + g\left(\frac{I_j}{I_j^*}\right) - g\left(\frac{I_k^* I_j S_k}{I_k I_j^* S_k^*}\right)\right) \right] \\ &\leq \sum_{k=1}^n v_k \left[\alpha_{k-1} I_{k-1}^* \left(g\left(\frac{I_{k-1}}{I_{k-1}^*}\right) - g\left(\frac{I_k}{I_k^*}\right)\right) + \sum_{j=1}^n \beta_{kj} S_k^* I_j^* \left(g\left(\frac{I_j}{I_j^*}\right) - g\left(\frac{I_k}{I_k^*}\right)\right) \right] \\ &= \sum_{k=1}^n v_k \left[\sum_{j=1}^n \left(\beta_{kj} S_k^* I_j^* + \delta_{k-1,j} \alpha_{k-1} I_{k-1}^* \right) \left(g\left(\frac{I_j}{I_j^*}\right) - g\left(\frac{I_k}{I_k^*}\right)\right) \right] \\ &= \sum_{k,j=1}^n v_k \phi_{kj}^* F_{kj}(I_k, I_j), \end{aligned}$$

where

$$F_{kj}(I_k, I_j) = g\left(\frac{I_j}{I_j^*}\right) - g\left(\frac{I_k}{I_k^*}\right), \quad 1 \leq j, k \leq n.$$

Let (\mathcal{G}, Φ) be the weighted digraph for the nonnegative matrix $\Phi = (\phi_{kj}^*)_{n \times n}$ and C be any directed cycle in \mathcal{G} , if one exists. Let $E(C)$ denote the set of edges of C . Then, the telescoping property of F_{kj} implies that

$$\sum_{(r,s) \in E(C)} F_{rs}(I_r, I_s) = 0.$$

It then follows from Theorems 2.2 and 3.1 in [21] that,

$$V'(t) \leq \sum_{k,j=1}^n v_k \phi_{kj}^* F_{kj}(I_k, I_j) = \sum_{Q \in Q} w(Q) \sum_{(r,s) \in E(C_Q)} F_{rs}(I_r, I_s) = 0,$$

for all $(S_1, I_1, S_2, I_2, \dots, S_n, I_n)$ in $\overset{\circ}{\Gamma}$. Here, Q is the set of all spanning unicyclic graphs of weighted digraph (\mathcal{G}, Φ) , $w(Q)$ is the weight of Q , and C_Q denotes the unique directed cycle in Q . Since $v_k > 0$, it can be verified that $V' = 0$ implies

$$S_k = S_k^*, \quad \text{and} \quad I_k = I_k^*, \quad k = 1, 2, \dots, n.$$

Therefore, the largest invariant set in $\overset{\circ}{\Gamma}$ on which $V'(t) = 0$ is the singleton $\{E^*\}$. By Lasalle's Invariance Principle [19], E^* is globally asymptotically stable in $\overset{\circ}{\Gamma}$. The global stability also implies that E^* is unique. \square

To demonstrate that our assumption (16) can be satisfied, and hence the results of Theorem 5 can hold, we carried out numerical simulations using a special case of model (4) with $n = 4$ and the following set of biologically plausible parameter values:

$$\Lambda_1 = 20, \quad \Lambda_2 = 150, \quad \Lambda_3 = 1200, \quad \Lambda_4 = 1550,$$

$$\mu = 0.0001, \quad \gamma = 0.01, \quad \alpha_1 = 0.004, \quad \alpha_2 = 0.005, \quad \alpha_3 = 0.006, \quad d_k = 0.001,$$

$$\beta_{1k} = \beta_{2k} = 0.24 \times 10^{-7}, \quad \beta_{3k} = 0.48 \times 10^{-7}, \quad \beta_{4k} = 0.16 \times 10^{-7}, \quad k = 1, 2, 3, 4.$$

The time unit in the simulations is week. With these values of parameters, it can be verified that the basic reproduction number $\mathcal{R}_0 = 5.2566 > 1$ and the threshold value $\mathcal{T}_0 = 4.9652 > 1$. Furthermore, $S_1^* = 1.97 \times 10^3$, $S_2^* = 1.42 \times 10^3$, $S_3^* = 7.35 \times 10^4$, and $S_4^* = 4.49 \times 10^5$. The coefficients $v_k = 456138.4$ for $k = 1, 2, 3, 4$. Expressions on the right hand side of (16) are

$$d_1 S_1^* + \alpha_1 S_1^* - \frac{v_2}{v_1} \alpha_1 S_1^* = 1.97 > 0, \quad (17)$$

$$d_2 S_2^* + \alpha_2 S_2^* - \alpha_1 S_1^* - \frac{v_3}{v_2} \alpha_2 S_2^* = 6.28 > 0, \quad (18)$$

$$d_3 S_3^* + \alpha_3 S_3^* - \alpha_2 S_2^* - \frac{v_4}{v_3} \alpha_3 S_3^* = 2.66 > 0, \quad (19)$$

$$d_4 S_4^* - \alpha_3 S_3^* = 8.33 > 0. \quad (20)$$

This shows that the assumption (16) is satisfied for an open set of the parameters values. Simulation results shown in Fig. 2 demonstrate that solutions with different initial values converge to positive equilibrium values in all four age groups.

In some special cases, assumption (16) can hold for all positive parameter values. In a large population, the number of susceptible people $\alpha_k S_k$ who transit into the next age group S_{k+1} each year is typically small compare to the sizes of S_k and S_{k+1} , since only people

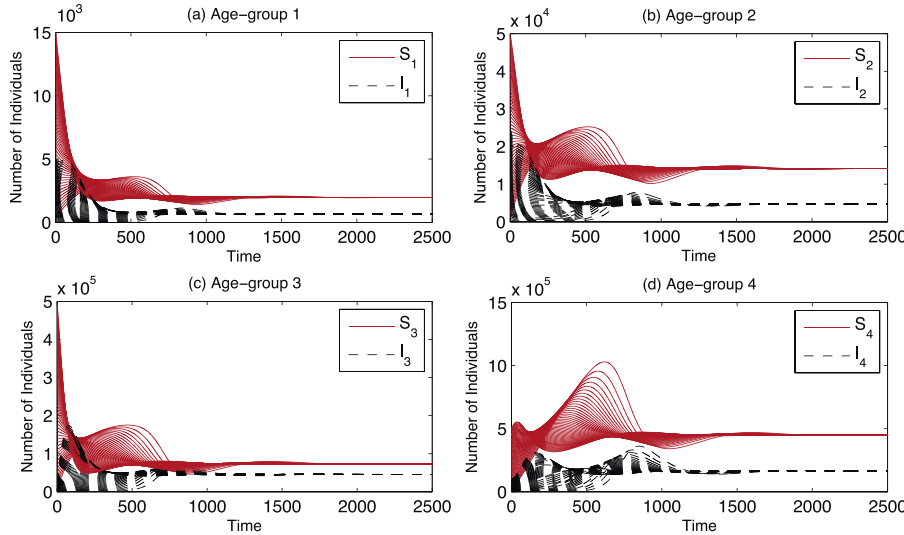


Fig. 2. Numerical simulations of a discrete age-structured epidemic model (4) with $n = 4$. The parameter values used for the simulations are $\Lambda_1 = 20$, $\Lambda_2 = 150$, $\Lambda_3 = 1200$, $\Lambda_4 = 1550$, $\mu_k = 0.0001$, $\gamma = 0.01$, $\alpha_1 = 0.004$, $\alpha_2 = 0.005$, $\alpha_3 = 0.006$, $\beta_{1k} = \beta_{2k} = 0.24 \times 10^{-7}$, $\beta_{3k} = 0.48 \times 10^{-7}$, $\beta_{4k} = 0.16 \times 10^{-7}$, and $d_k = 0.001$, $k = 1, 2, 3, 4$. The basic reproduction number $\mathcal{R}_0 = 5.25667 > 1$. The figures demonstrate that solutions with different initial values converge to positive equilibrium values in all four age groups.

whose age is the highest in S_k will transfer into S_{k+1} . The impact of aging of susceptibles $\alpha_k S_k$ on the incidence in the $(k+1)$ th age group $\beta_{kj} \alpha_{k-1} S_{k-1} I_j$ is typically small. In the following, we assume that changes in S_{k+1} due to the aging term $\alpha_k S_k$ are negligible with respect to its impact on the disease incidence. We then arrive at the following simplified model:

$$\begin{aligned} \frac{dS_k}{dt} &= \Lambda_k - \sum_{j=1}^n \beta_{kj} S_k I_j - d_k S_k, \\ \frac{dI_k}{dt} &= \alpha_{k-1} I_{k-1} + \sum_{j=1}^n \beta_{kj} S_k I_j - (d_k + \mu_k + \gamma_k + \alpha_k) I_k, \end{aligned} \quad k = 1, 2, \dots, n. \quad (21)$$

Since the matrices F , V in the calculation of \mathcal{R}_0 do not depend on the equations for the susceptible populations, the basic reproduction number for the revised model is given by $\mathcal{R}_0 = \rho(FV^{-1})$, where F and V are the same as given in (6) with $S_k^0 = \Lambda_k/d_k$, $k = 1, 2, \dots, n$. For model (21), terms $\alpha_k S_k^*$ in (16) vanish, and thus assumption (16) holds automatically. We have the following result.

Theorem 6. Assume $B = (\beta_{kj})_{n \times n}$ is irreducible. Suppose that the basic reproduction number for system (21) satisfies $\mathcal{R}_0 > 1$. Then there exists a unique endemic equilibrium $E^* = (S_1^*, I_1^*, \dots, S_n^*, I_n^*)$, and E^* is globally asymptotically stable in Γ .

4. An application to vaccination strategies for measles

Measles is a vaccine preventable disease. Given as part of the measles-mumps-rubella (MMR) vaccine, the measles vaccine typically requires two doses. The first dose of measles containing vaccine (MCV1) is commonly given to infants at 12 or 15 months of age, and it has an efficacy between 85% and 93%. A second dose (MCV2) is recommended to be given before school age. With two doses, the efficacy of MCV can reach as high as 97% [30,31]. In the United States and other developed countries, where measles have been under control, the coverage rate of MCV1 among children is well over 90%, while the

MCV1 global coverage rate has stagnated around 85% and much lower in many developing countries. According to WHO's guidelines for introducing the second dose of measles vaccine [36], when MCV1 coverage in a country/region has been higher than 80% for three consecutive years, MCV2 should be administered to children either at the age of 15–18 months or at the school entry, depending on which choice will enable a higher vaccination coverage. In this section, we develop a two-dose vaccination model with four age groups (Fig. 3) to study the vaccination strategies for measles epidemics and apply the model to analyze measles data from India, one of the countries with highest measles incidence in the world.

4.1. Measles vaccination model for India

Measles vaccine has been licensed and introduced nationally in India since 1985 [17]. A single dose is administered to children at 9 months of age. The vaccination coverage has been low in the early stage of the vaccination programme and has reached 80% since 2010 [39]. Starting from 2010, the Indian Academy of Pediatrics (IAP) recommended two doses of MMR vaccine, MCV1 at 15–18 months and MCV2 at school entry (4–6 years of age) [5,15,16]. Measles case mortality rate varies drastically among different age groups; it is the highest among children 4 years of age and younger, the next highest among children aged 5–9 years, and the case mortality rate is very small among children older than 10 years. Based on consideration of age-specific differences in vaccination schedules, case fatality rates, and contact patterns, we partition the host population into the following four age groups:

- infants (0 – 4 years), children (5 – 9 years), teenagers (10 – 14 years), and the rest (15+ years).

The model structure is illustrated in the transfer diagram in Fig. 3. Compared to the general model structure in Fig. 1, we have incorporated a two-dose measles vaccination: MCV1 for age group 1 and MCV2 for age group 2. The model is described by the following system of differential equations:

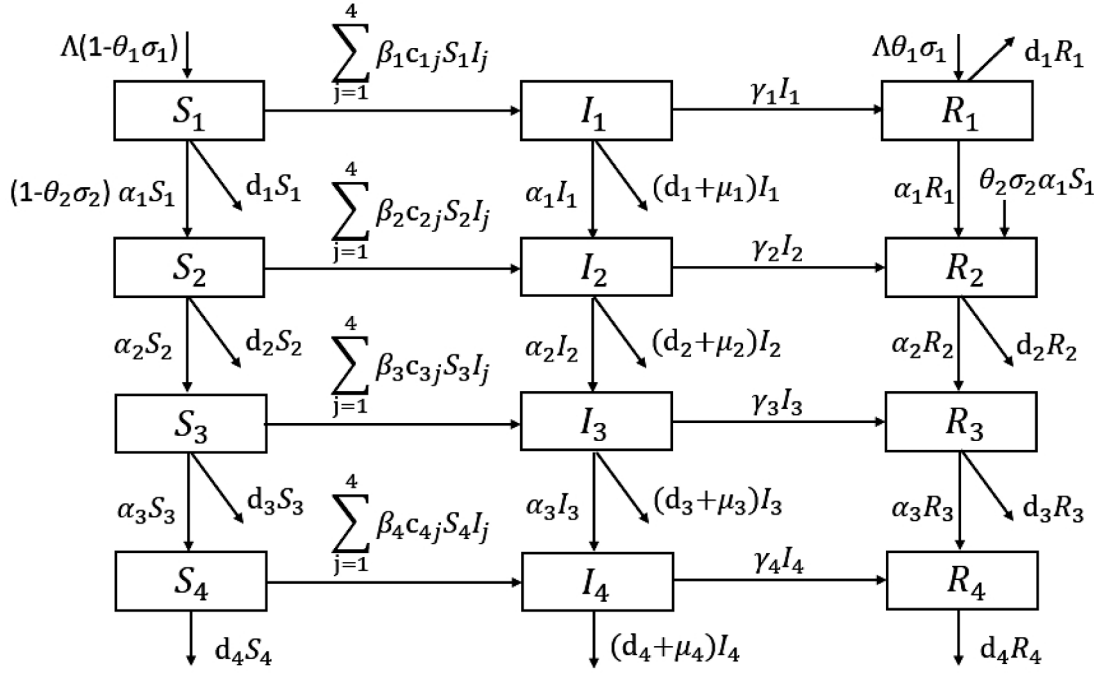


Fig. 3. Transfer diagram for a vaccination model with four age groups.

$$\begin{aligned}
 \frac{dS_1}{dt} &= (1 - \theta_1\sigma_1)\Lambda - \sum_{j=1}^4 \beta_1 c_{1j} S_1 I_j - d_1 S_1 - \alpha_1 S_1, \\
 \frac{dI_1}{dt} &= \sum_{j=1}^4 \beta_1 c_{1j} S_1 I_j - (d_1 + \mu_1 + \gamma_1 + \alpha_1) I_1, \\
 \frac{dR_1}{dt} &= \theta_1\sigma_1\Lambda + \gamma_1 I_1 - d_1 R_1 - \alpha_1 R_1, \\
 \frac{dS_2}{dt} &= (1 - \theta_2\sigma_2)\alpha_1 S_1 - \sum_{j=1}^4 \beta_2 c_{2j} S_2 I_j - d_2 S_2 - \alpha_2 S_2, \\
 \frac{dI_2}{dt} &= \alpha_1 I_1 + \sum_{j=1}^4 \beta_2 c_{2j} S_2 I_j - (d_2 + \mu_2 + \gamma_2 + \alpha_2) I_2, \\
 \frac{dR_2}{dt} &= \alpha_1 R_1 + \theta_2\sigma_2\alpha_1 S_1 + \gamma_2 I_2 - d_2 R_2 - \alpha_2 R_2, \\
 \frac{dS_3}{dt} &= \alpha_2 S_2 - \sum_{j=1}^4 \beta_3 c_{3j} S_3 I_j - d_3 S_3 - \alpha_3 S_3, \\
 \frac{dI_3}{dt} &= \alpha_2 I_2 + \sum_{j=1}^4 \beta_3 c_{3j} S_3 I_j - (d_3 + \mu_3 + \gamma_3 + \alpha_3) I_3, \\
 \frac{dR_3}{dt} &= \alpha_2 R_2 + \gamma_3 I_3 - d_3 R_3 - \alpha_3 R_3, \\
 \frac{dS_4}{dt} &= \alpha_3 S_3 - \sum_{j=1}^4 \beta_4 c_{4j} S_4 I_j - d_4 S_4, \\
 \frac{dI_4}{dt} &= \alpha_3 I_3 + \sum_{j=1}^4 \beta_4 c_{4j} S_4 I_j - (d_4 + \mu_4 + \gamma_4) I_4, \\
 \frac{dR_4}{dt} &= \alpha_3 R_3 + \gamma_4 I_4 - d_4 R_4.
 \end{aligned} \tag{22}$$

Model parameters, together with their meaning and estimated values, are given in Table 1. In particular, θ_1 and θ_2 are vaccination rate of MCV1 and MCV2, respectively, and σ_1 and σ_2 are the respective efficacies of MCV1 and MCV2, so that $\sigma_1\theta_1$ and $\sigma_2\theta_2$ are the effective coverage of MCV1 and MCV2, respectively. The transmission coefficient β_{kj} between S_k and I_j is decomposed into two factors: $\beta_{kj} = \beta_k c_{kj}$, where β_k is the probability of transmission for an average contact between a susceptible individual in age group k (S_k) with an infected individual, and c_{kj} is the average number of contacts from individuals in age groups

j with individuals in age group k . We note that c_{kj} and c_{jk} may not be the same due to different sizes of age groups, and the contact matrix (c_{ij}) may not be symmetric. Other parameters have the same meaning as in the general model (1).

4.2. Parameters estimation and model calibration

As indicated in Table 1, values of some parameters and initial values of state variables in model (22) are estimated directly from published data. We have followed the procedure in [23,24] to compute the contact matrix (c_{ij}) for the population of India, using population data to derive age distributions among the four age groups. The result is shown in Table 2. Other parameter values, especially those of the probability of transmission per contact (β_i) and the recovery rate from measles (γ_i) for each age group, are estimated by fitting the model outcomes to measles data using the nonlinear least squares method [10]. The measles data used for model fitting include the reported annual incidence and age specific incidence of measles in India from 2000 to 2010 [26,39,40]. The values of measles case-fatality-ratio (CFRs) are $\mu_1 = 0.016$, $\mu_2 = 0.08$, $\mu_3 = \mu_4 = 0$ [26]. By the end of 2015, the values of θ_1 , θ_2 are the actual vaccination rates published by WHO, and we assume that $\theta_1 = 0.85$ and $\theta_2 = 0.8$ from 2016 onwards. In Figs. 4 and 5, we provide a comparison between the model simulations using the estimated parameter values and the reported annual incidence of India from 2011 to 2015 for the total population and four age groups [39,40]. These figures show a good fit between our model predictions and the data.

4.3. Immune profile analysis

Our calibrated model is used to generate the measles immune profiles for the total population and for different age groups. The baseline is the current measles vaccination policy in India, namely, a single-dose (MCV1) for the first age group of children (4 years and younger) during years 2000–2010, and a second dose (MCV2) after 2010 for the second age group of children (5–9 years olds). We assume that the vaccination coverage of the first dose is 85% ($\theta_1 = 0.85$) and that of the second dose 80% ($\theta_2 = 0.8$). The efficacy of the first dose is 85% ($\sigma_1 = 0.85$) and that of the second dose 95% ($\sigma_2 = 0.95$). The results are shown in Fig. 6.

Table 1
Parameters and their estimated values for model (22).

| Parameter | Value/Range | Unit | Definition | Reference |
|------------|---------------------------|--------------------|--|------------|
| Λ | 650 | $10^3/\text{week}$ | Influx of susceptibles | Fitting |
| d_k | 0.00029 | week^{-1} | Natural mortality rate of age group k | [37] |
| α_k | 0.00385 | week^{-1} | Aging rate of age group k | Calculated |
| γ_k | 0.024368 | week^{-1} | Recovery rate of age group k | Fitting |
| μ_k | [0,0.2] | | Case fatality rate of age group k | [26] |
| θ_k | [0,1] | | Immunization rate of Measles vaccine | [38] |
| σ_1 | 0.85 | | Efficacy of MCV1 | [12,25] |
| σ_2 | 0.95 | | Efficacy of MCV2 | [30] |
| β_1 | 0.167989×10^{-6} | | Probability of transmission per contact for age group 1 | Fitting |
| β_2 | 0.515425×10^{-7} | | Probability of transmission per contact for age group 2 | Fitting |
| β_3 | 0.262981×10^{-7} | | Probability of transmission per contact for age group 3 | Fitting |
| β_4 | 0.285701×10^{-8} | | Probability of transmission per contact for age group 4 | Fitting |
| c_{kj} | See Table 2 | week^{-1} | Average number of contacts from age group j to age group k | [24] |

Note: $k, j = 1, 2, 3, 4$.

Table 2
Contact matrix for model (22).

| | 0–4 years | 5–9 years | 10–14 years | 15+ years |
|-------------|-----------|-----------|-------------|-----------|
| 0–4 years | 13.3 | 5.88 | 3.08 | 27.65 |
| 5–9 years | 6.02 | 46.2 | 8.26 | 38.29 |
| 10–14 years | 3.22 | 8.54 | 48.3 | 37.94 |
| 15+ years | 4.41 | 6.02 | 5.74 | 73.5 |

In Fig. 6(a), the immune profile for the total population is shown. With India's sustained effort on measles immunization programmes, especially after the introduction of MCV2 in 2010, the fraction of population that are protected by immunity has been increasing, albeit slowly during 2000–2010. The fraction of population that are protected by vaccination has increased drastically after 2010 and surpassed the fraction who are protected by immunity due to past infection. This demonstrated the effectiveness of the MCV2 at the population level.

Fig. 6(b)–(d) show the immune profiles in each of the four age groups. The proportion of population who are protected by immunity in the first three age groups are much higher than that in the whole population, which is estimated at 55% in 2016. For infants aged 0–4 years, this proportion is estimated at 70% in 2016. Because of the introduction

of MCV2 to the second age group (5–9 years), proportion of the immune population in that age group is the highest at an estimated level of 75%. This shows that MCV2 is highly effective for increased protection of the targeted age group.

The model also allows us to project the level of immunity in the populations beyond year 2016. As shown in Fig. 6(a), proportion of the immune population will reach 65% by the end of 2025, which is still significantly below the WHO target of 95%, which is the level required for herd immunity for measles [1]. This proportion will be much higher in the vaccine targeted age groups. For children aged 5–9 years, the proportion of the population with immunity against measles will be over 90% at the end of 2025, and the corresponding proportion among children aged 10–14 years will be 85%, due to aging of children who were vaccinated at a younger age. In contrast, for children 4 years of age and younger, the immune proportion will only reach a low rate of 72% by the end of 2025.

Our model projections show that the current two-dose policy of measles vaccination programme in India had a great effect on increasing the proportion of immune individuals among children aged 5–14 years. In Fig. 7, our model projections also show a drastic decline in measles mortality rates among children 9 years of age and younger during 2016–2025. In Fig. 8(a), the solid curve is our projection of the

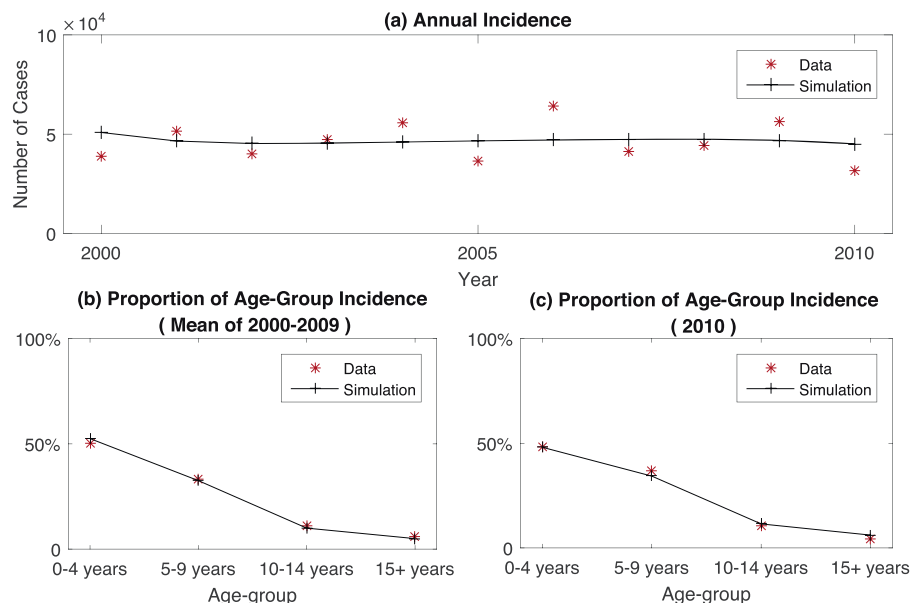


Fig. 4. Model fitting results. Using the nonlinear least-squares method, reported annual incidence and age-specific incidence of India from 2000 to 2010 [26,39,40] are used to estimate the transmission coefficients β_k , recovery rate γ_k and the initial values of the infected individuals I_k for $k = 1, 2, 3, 4$.

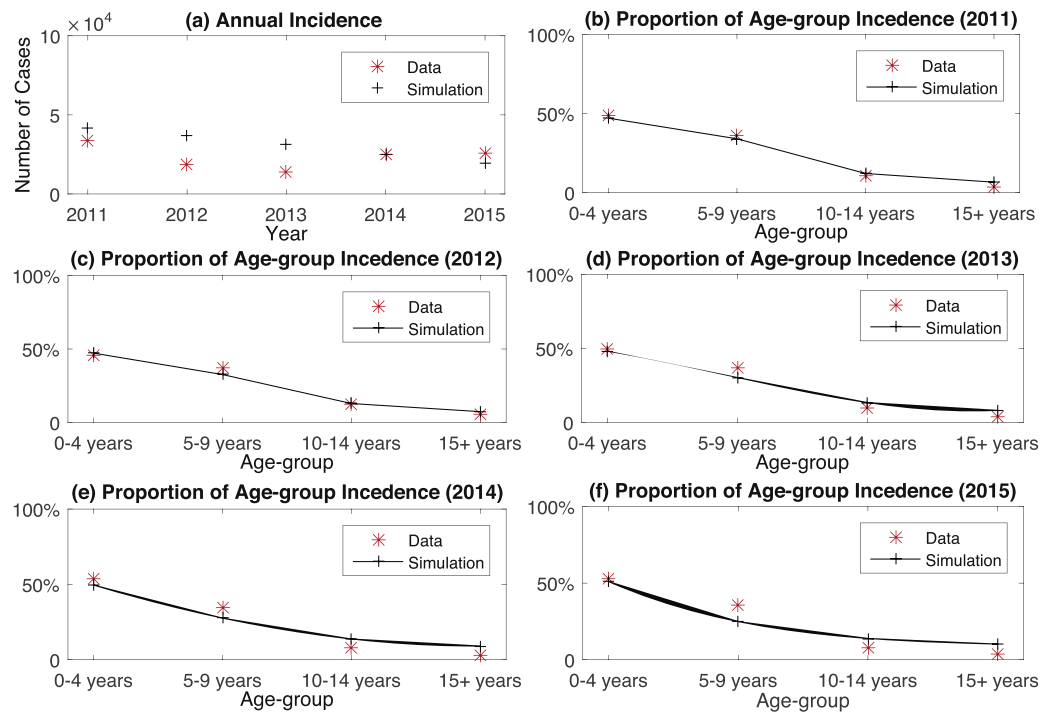


Fig. 5. Reported annual measles incidence in total population and in four age groups of India from 2011 to 2015 [39,40] compared to the simulation results of the calibrated model.

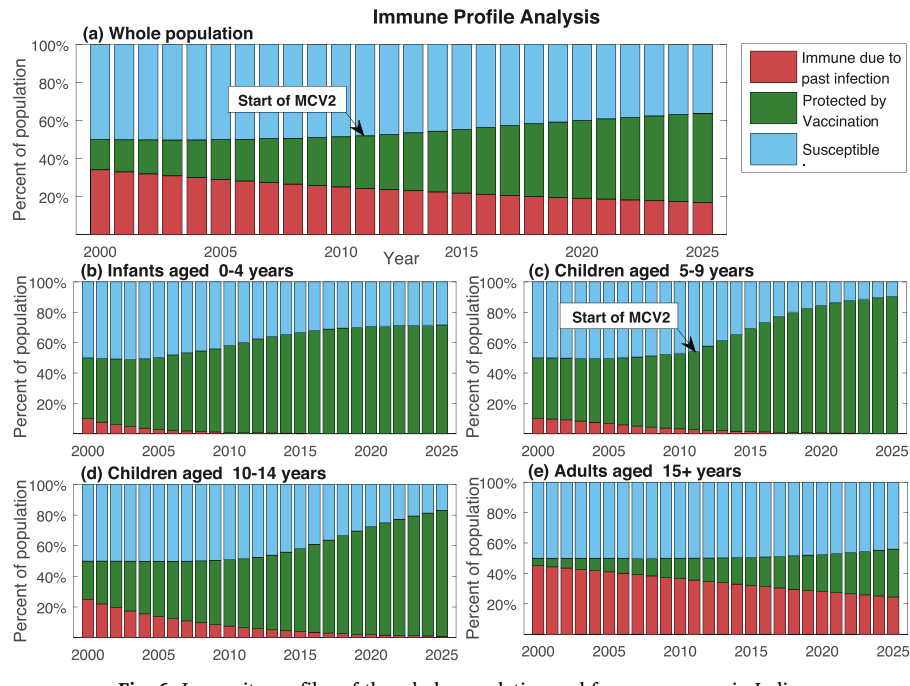


Fig. 6. Immunity profiles of the whole population and four age groups in India.

decline in measles annual incidence for the whole population of India during 2016–2025.

Despite these positive effects of the current vaccination programme in India, our model projection shows that (the solid line in Fig. 8(a)), by the end of 2020, the India's annual measles incidence rate in 2020 will remain above the WHO elimination goal of 5 cases per one million population. From our immune profile analysis in Fig. 6, we can see that part of the reason lies in the low effective coverage rate of MCV1 ($\theta_1 \cdot \sigma_1$) among children aged 0–4 years, which will only be at 72.25% in year 2020. This age group has the highest proportion of the measles incidence during 2000–2010 (Fig. 4). The effective coverage rate of

MCV1 ($\theta_1 \cdot \sigma_1$) can be boosted by increasing the vaccine coverage rate θ_1 or increasing the vaccine efficacy σ_1 . We discuss the effects of these two strategies in the next two sections.

4.4. Effect of increasing measles vaccination coverage

According to the recommendation of WHO, coverages of MCV1 and MCV2 should both be increased to 95%. We explored several scenarios in which the coverage rate of MCV1 or MCV2 are increased to 95%. Results are shown in Figs. 8 and 9.

In Fig. 8(a), we compared the two scenarios of increasing coverage

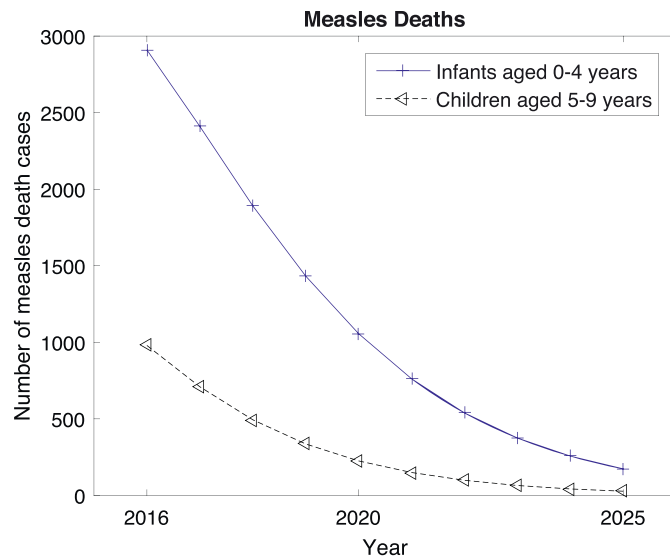


Fig. 7. Measles deaths in infants aged 0–4 years and in children aged 5–9 years.

rate θ_1 of MCV1 or θ_2 of MCV2 starting from 2016, while keeping the vaccine efficacies the same as in Table 2. Our results show that a 10% increase in MCV1 coverage rate (θ_1) can be more effective in reducing the measles cases than a 15% increase in MCV2 coverage rate (θ_2). This is partly because of the relative low coverage rate of MCV1 in the baseline.

In Fig. 9, we show that the proportion of annual measles incidence coming from first age group continues to rise during 2016–2020, under different scenarios of scaling up vaccine coverages. As the annual incidence of the entire population continues to decline, larger and larger proportion of the measles cases will come from children 4 years of age and younger. Combined with the fact that the measles fatality rate is the highest in this age group, our model projections indicate that a good alternative strategy for measles control in India is to give priority to boost the coverage rate of measles vaccination MCV1 among children of age 0–4 years.

4.5. Effects of improving efficacy of measles vaccines

In the United States and other developed countries, the efficacy of

MCV1 can reach 95% when administered to children of age 12 months and older [29]. In India, MCV1 is administered to children of age 15–18 months, with an efficacy of 85% [12,25]. There is room for India to increase the efficacy of MCV1. We explore the scenario of increasing the efficacy of MCV1 (σ_1) from the current 85% to 95%. Results are shown in Fig. 9.

Our projections show that increasing the efficacy of MCV1 by 10% has a strong effect on reducing the measles incidence in all combinations of coverage rates of MCV1 and MCV2 we have examined. In particular, if the efficacy of MCV1 and MCV2 can both reach 95%, the annual measles incidence can be reduced to below 5 cases per million in 2020 even with a coverage rate 85% for MCV1 and 80% for MCV2 (Fig. 9(b)), allowing India to reach WHO's measles elimination target.

5. Conclusions and discussion

In this paper, we investigated the global dynamics of a class of epidemic models with discrete age structure (4). We have derived the basic reproduction number \mathcal{R}_0 for the model and show that it is a sharp threshold. More specifically, if $\mathcal{R}_0 \leq 1$, the disease-free equilibrium E_0 is globally asymptotically stable, and if $\mathcal{R}_0 > 1$ and the transmission matrix $\{\beta_{ij}\}$ among age groups is irreducible, then the endemic equilibrium E^* is unique and globally asymptotically stable, under a mild condition. While this is a new result, the complete resolution of the uniqueness and global stability of the endemic equilibrium of epidemic models with a discrete age structure still remains open.

We applied our discrete age-structured epidemic model to study the effectiveness of vaccination strategies for measles in India, in the context of WHO's Global Measles and Rubella Strategic Plan: 2012–2020, and its measles eradication targets for year 2020 for high measles incidence countries in Africa and Southeast Asia. We have calibrated a measles vaccination model (22) with four age groups that incorporated the current measles vaccination programmes (MCV1 and MCV2) in India, using published measles surveillance data from India [26,39,40]. We used our model to analyze the immune profile in the whole population and in each age groups to establish the baseline and make future projections. Our model projections show that, due to a low MCV1 coverage among children of age 0–4 years at 70% in 2020 if the current vaccination programmes are to continue, India will not likely to reach the WHO's measles eradication target for 2020.

We have also used our calibrated model to explore alternative measles vaccination strategies such as increasing the vaccine coverage

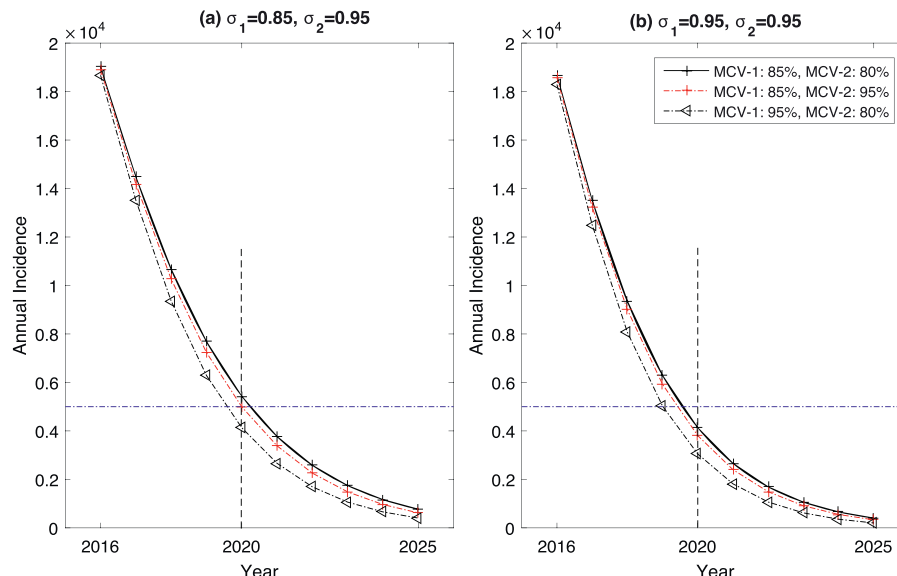


Fig. 8. Effect of increased vaccination coverage (MCV1/MCV2) and improved efficacy of measles vaccine.

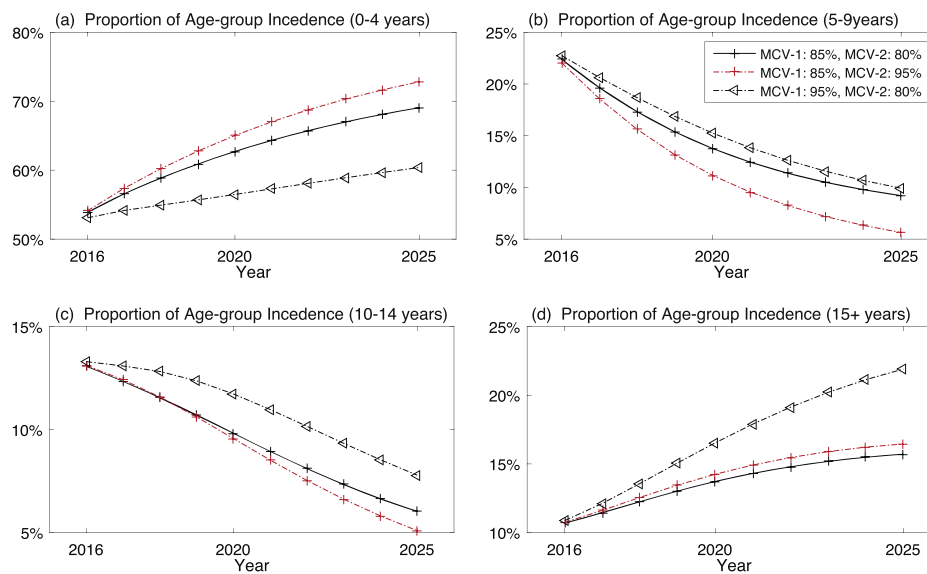


Fig. 9. Percentage of the total measles incidence from four age groups under three different sets of vaccination coverage.

of MCV1 or MCV2, and increasing vaccine efficacy of MCV1. Our model predictions show that increasing the coverage rate of MCV1 among children of age 0–4 years is more effective than increasing the coverage rate of MCV2 for children of age 5–9 years. We also show that increasing the efficacy of MCV1 can be most effective in reducing the measles incidence even at a moderate vaccine coverage rate. With a coverage rate 85% for MCV1 and 80% for MCV2, increasing vaccine efficacy from the current 85% to 95% will allow India to reduce the annual measles incidence rate to below 5 cases per one million population by 2020, reaching WHO's measles eradication target for measles incidence reduction.

Our results in this paper demonstrated the utility of discrete age-structured epidemic model for analyzing vaccination strategies for measles. Similar analysis can be adapted to study control strategies for other infectious diseases. There is a great potential for discrete age-structured models in cost-effectiveness analysis of vaccination strategies.

Funding

LZ and YW acknowledge the support of China Scholarship Council for their visits to the University of Alberta, where this work was carried out. YX acknowledges the support of Simon Foundations. Research of MYL is supported in part by grants from the Natural Sciences and Engineering Research Council of Canada (NSERC) RGPIN 05395-Li and Canada Foundation for Innovation (CFI) New Opportunities 7112.

Supplementary material

Supplementary material associated with this article can be found, in the online version, at doi:[10.1016/j.mbs.2018.12.003](https://doi.org/10.1016/j.mbs.2018.12.003).

References

- [1] R.M. Anderson, R.M. May, Immunisation and herd immunity, *Lancet* 335 (1990) 641–645.
- [2] R.M. Anderson, R.M. May, *Infectious Diseases of Humans: Dynamics and Control*, Oxford University Press, 1992.
- [3] V. Andreasen, Instability in an SIR-model with age-dependent susceptibility, in: O. Arino, D. Axelrod, M. Kimmel, M. Langlais (Eds.), *Mathematical Population Dynamics*, Winnipeg: Wuerz Publishers, 1995, pp. (3–14).
- [4] A. Berman, R.J. Plemmons, *Nonnegative Matrices in the Mathematical Sciences*, SIAM, 1994.
- [5] N. Bhattacharjee, R. Kaur, M. Gupta, et al., Introducing combined measles, mumps and rubella vaccine in Chandigarh, India: issues and concerns, *Indian Pediatr.* 51 (2014) 441–443.
- [6] N.P. Bhatia, G.P. Szegö, *Dynamical Systems: Stability Theory and Applications*, Springer, 2006.
- [7] O. Diekmann, J.A.P. Heesterbeek, *Mathematical epidemiology of infectious diseases: model building, analysis and interpretation*, Wiley Series in Mathematical and Computational Biology, Wiley & Sons, 2000.
- [8] A. Franceschetti, A. Pugliese, Threshold behaviour of a SIR epidemic model with age structure and immigration, *J. Math. Biol.* 57 (2008) 1–27.
- [9] H.I. Freedman, S. Ruan, M. Tang, Uniform persistence and flows near a closed positively invariant set, *J. Dyn. Differ. Equ.* 6 (1994) 583–600.
- [10] D.M. Glover, W.J. Jenkins, S.C. Doney, Least squares and regression techniques, goodness of fit and tests, non-linear least squares techniques, *Modeling Methods for Marine Science*, Cambridge University Press, 2008, pp. 49–74.
- [11] H.H. Guo, M.Y. Li, Z. Shuai, Global stability of the endemic equilibrium of multi-group SIR epidemic models, *Can. Appl. Math. Q.* 14 (2006) 259–284.
- [12] S.K. Gupta, S. Sosler, P. Haldar, et al., Introduction strategy of a second dose measles containing vaccine in India, *Indian Pediatr.* 48 (2011) 379–382.
- [13] H.W. Hethcote, The mathematics of infectious diseases, *SIAM Rev.* 42 (2000) 599–653.
- [14] R.A. Horn, C.R. Johnson, *Matrix Analysis*, Cambridge University Press, 2012.
- [15] I.A.O. P. (IAP), Recommended immunization schedule for children aged 0 through 18 years-India, 2016 and updates on immunization, <http://acvip.org/files/IAP-immunization-schedule-2016-IP-2016-Epub.pdf> (accessed on April 16, 2017).
- [16] I.A.O. Pediatrics, IAP guide book on immunization, 2011, 2011 <http://www.iapindia.org/files/IAP> (accessed on April 16, 2017).
- [17] T.J. John, V.P. Vergheze, Time to re-think measles vaccination schedule in India, *Indian J. Med. Res.* 134 (2011) 256–259.
- [18] T. Kuniya, Global stability analysis with a discretization approach for an age-structured multigroup SIR epidemic model, *Nonlinear Anal.* 12 (2011) 2640–2655.
- [19] J.P. LaSalle, *The Stability of Dynamical Systems*, SIAM, 1976.
- [20] M.Y. Li, J.R. Graef, L. Wang, et al., Global dynamics of an SEIR model with varying total population size, *Math. Biosci.* 160 (1999) 191–213.
- [21] M.Y. Li, Z. Shuai, Global-stability problem for coupled systems of differential equations on networks, *J. Differ. Equ.* 248 (2010) 1–20.
- [22] M. Martcheva, *An Introduction to Mathematical Epidemiology*, Springer, New York, 2015.
- [23] M.I. Meltzer, M. Gambhir, C.Y. Atkins, et al., Standardizing scenarios to assess the need to respond to an influenza pandemic, *Clin. Infect. Dis.* 60 (2015) S1–S8.
- [24] J. Mossong, N. Hens, M. Jit, et al., Social contacts and mixing patterns relevant to the spread of infectious diseases, *PLoS Med.* 5 (2008). E74.
- [25] M.V. Murhekar, Y.J. Hutin, R. Ramakrishnan, et al., The heterogeneity of measles epidemiology in India: implications for improving control measures, *J. Infect. Dis.* 204 (2011) S421–S426.
- [26] E. Simons, M. Ferrari, J. Fricks, et al., Assessment of the 2010 global measles mortality reduction goal: results from a model of surveillance data, *Lancet* 379 (2012) 2173–2178.
- [27] H.L. Smith, P. Waltman, *The Theory of the Chemostat: Dynamics of Microbial Competition*, Cambridge University Press, 1995.
- [28] H.R. Thieme, Stability change of the endemic equilibrium in age-structured models for the spread of S-I-R type infectious diseases, in: S. Busenberg, M. Martelli (Eds.), *Differential Equations Models in Biology, Epidemiology and Ecology*. Lecture Notes in Biomathematics, 92 Springer, Berlin, Heidelberg, 1991.
- [29] U.S. CDC, Immunization of health-care personnel: recommendations of the advisory committee on immunization practices (ACIP), *MMWR Recomm. Rep.* 60 (2011) 1–45. <https://www.cdc.gov/mmwr/preview/mmwrhtml/rr6007a1.htm> (accessed on April 16, 2017).

- [30] U.S. CDC, Measles vaccination, <https://www.cdc.gov/measles/vaccination.html> (accessed on April 16, 2017).
- [31] U.S. CDC, Recommended immunization schedules for persons aged 0 through 18 years, <http://www.cdc.gov/vaccines/schedules/downloads/child/0-18yrs-child-combined-schedule.pdf> (accessed on April 16, 2017).
- [32] P. van den Driessche, J. Watmough, Reproduction numbers and sub-threshold endemic equilibria for compartmental models of disease transmission, *Math. Biosci.* 180 (2002) 29–48.
- [33] W.H. Organization, Measles fact sheet, march 2017, <http://www.who.int/mediacentre/factsheets/fs286/en/> (accessed on April 16, 2017).
- [34] W.H. Organization, Global measles and rubella strategic plan: 2012–2020, http://apps.who.int/iris/bitstream/10665/44855/1/9789241503396_eng.pdf (accessed on April 16, 2017).
- [35] W.H. Organization, Measles elimination, http://www.who.int/immunization/sage/meetings/2015/october/8_GVAP_Secretariat_report_2015_Measles.pdf (accessed on April 16, 2017).
- [36] W.H. Organization, A guide to introducing a second dose of measles vaccine into routine immunization schedules, 2013, http://apps.who.int/iris/bitstream/10665/85900/1/WHO_IVB_13.03_eng.pdf (accessed on April 16, 2017).
- [37] W.H. Organization, Global health observatory (GHO) data: India, http://www.who.int/gho/countries/ind/country_profiles/en/ (accessed on April 16, 2017).
- [38] WHO/UNICEF, National immunization coverage, http://www.who.int/immunization/monitoring_surveillance/routine/coverage/en/index4.html (accessed on April 16, 2017).
- [39] W.H. Organization, Vaccine-preventable diseases: monitoring system, http://apps.who.int/immunization_monitoring/globalsummary/countries?countrycriteria (accessed on April 16, 2017).
- [40] W.H. Organization, EPI fact sheet: India, 2016, <http://www.searo.who.int/entity/immunization/data/india.pdf> (accessed on April 16, 2017).